



Detection of contaminated hazelnuts and ground red chili pepper flakes by multispectral imaging

H. Kalkan^{a,c,*}, P. Beriat^a, Y. Yardimci^a, T.C. Pearson^b

^a Middle East Technical University, Ankara, Turkey

^b USDA-ARS-CGAHR, Manhattan, KS, USA

^c Suleyman Demirel University, Isparta, Turkey

ARTICLE INFO

Article history:

Received 20 July 2010

Received in revised form 2 February 2011

Accepted 20 March 2011

Keywords:

Multispectral imaging

Food safety

Feature extraction

Classification

ABSTRACT

Mycotoxins are the toxic metabolites of certain filamentous fungi and have been demonstrated to cause various health problems in humans, including immunosuppression and cancer. Among them, the aflatoxins have received greater attention because they are potent carcinogens and are responsible for many human deaths per annum, mostly in non-industrialized countries. Various regulatory agencies have enforced limits on the concentrations of these toxins in foods and feeds involved in international commerce. Hyperspectral and multispectral imaging are becoming increasingly important for rapid and non-destructive testing for the presence of such contaminants. However, the high number of spectral bands needed may render such image acquisition systems too complex, expensive and slow. Moreover, they tend to generate overwhelming amount of data, making effective processing of this information in real time difficult. In this study, a two-dimensional local discriminant bases algorithm was developed to detect the location of the discriminative features in the multispectral data space. The algorithm identifies the optimal passband width and center frequencies of optical filters to be used for a multispectral imaging system. This was applied to a multispectral imaging system used to detect aflatoxin-contaminated hazelnut kernels and red chili peppers. Classification accuracies of 92.3% and 80% were achieved for aflatoxin-contaminated and uncontaminated hazelnuts and red chili peppers, respectively. The aflatoxin concentrations were decreased from 608 to 0.84 ppb for tested hazelnuts and from 38.26 to 22.85 ppb for red chili peppers by removal of the nuts/peppers that were classified as aflatoxin-contaminated. The algorithm was also used to classify fungal contaminated and uncontaminated hazelnut kernels, and an accuracy of 95.6% was achieved for this broader classification.

© 2011 Elsevier B.V. All rights reserved.

1. Introduction

Food items are infected by various types of fungi during growth, harvesting, drying, possessing and storage, resulting in mycotoxin formation. There are over 300 different mycotoxin species, and most of them are produced by *Aspergillus*-, *Penicillium*-, *Fusarium*-, *Alternaria*-, *Cladosporium*- and *Rhizopus*-type fungi. *Aspergillus* fungi can produce aflatoxins that are associated with toxicity and carcinogenicity in animals (Dichter, 1984). Due to aflatoxin's carcinogenic effects and frequent occurrence in agricultural products, its concentration in foods is restricted by regulations. The allowed aflatoxin levels in Europe for seeds and spices are 4 and 10 ppb, respectively (European Commission Regulation, 2006). The corresponding aflatoxin limit is 20 ppb for all food items traded in USA and Turkey. All consumed and exported foods are expected to fulfill these limits. Currently, the aflatoxin contamination of a

* Corresponding author at: Suleyman Demirel University, Isparta, Turkey. Tel.: +90 246 211 1392; fax: +90 246 237 0859.

E-mail address: habilkalkan@sdu.edu.tr (H. Kalkan).

food lot is determined by chemically analyzing the samples taken from the lot. However, aflatoxin contamination is highly heterogeneous, and contaminated seeds are often unevenly distributed (Schatzki and Pan, 1996). Therefore, it is more appropriate to detect and remove these contaminated seeds by non-invasive methods instead of discarding the entire lot.

Several methods have been developed to measure the fungal or toxin contamination non-invasively. Spectrophotometers have been used to identify aflatoxin contamination by detecting symptoms of fungal damage to food items. A spectrometer measures reflected (R) or transmitted (T) light at various spectral bands. Near infrared (NIR) frequency bands can be used for food safety inspections. Pearson et al. (2001) used the spectral reflectance ratio (R735/R1005 nm) for distinguishing highly contaminated corn kernels (>100 ppb) from those contaminated below 10 ppb and reached a 95% correct classification rate. They could also identify the highly contaminated (>100 ppb) yellow corn kernels at a rate of 98% with spectral absorbance at 750 and 1200 nm. Hirano et al. (1998) used the transmittance ratio (T700/T1100 nm) to identify contaminated peanut kernels among uncontaminated ones. However, the

acquisition of the complete spectrum from a spectrophotometer is time consuming and requires expensive instruments.

In addition to the NIR frequency bands, the bright greenish-yellow fluorescence (BGYF) test is a simple and widely used method for the detection of aflatoxin contaminated food items (Bollenbacher and Marsh, 1954). The fluorescence is produced by the reaction of peroxidases in living plants with kojic acid, which is formed by *Aspergillus types* (Marsh et al., 1969) or other fungi (Jacks, 2005). The number of exhibited BGYF particles is taken as an indication of aflatoxin contamination. The BGYF test is used to detect aflatoxin-contaminated pecans (Tayson and Clark, 1974), corn (Wicklow, 1999), figs (Steiner et al., 1988; Doster and Michailides, 1998), pistachios, Brazil nuts (Hadavi, 2005 and Steiner et al., 1992) and other contaminated agricultural commodities (Bothast and Hesselatine, 1975). Several spectral bands, including the 420, 440, 450 and 490 nm bands, were utilized individually to measure the BGY fluorescence (Tayson and Clark, 1974; Fersaie et al., 1978). However, Wilson (1989) found that aflatoxin-contaminated corn kernels do not always exhibit BGYF due to the insufficient amount of peroxidase in kernels. Moreover, other types of fungi that do not produce aflatoxin may yield kojic acid in foods and may be classified as aflatoxin-contaminated by the BGYF test (Jacks, 2005). Therefore, more advanced techniques should be utilized to obtain the spectral bands that include more discriminative information.

The determination of the best spectral bands to be used for contaminated foodstuffs is an important problem that spectroscopy and spectral imaging may help to solve with more research efforts. The collection of whole spectra or several images at different spectral bands is a simple matter in a laboratory setting with limited, stationary samples. Collecting spectra or multispectral images on moving products in a food processing stream and performing analysis and sorting of the product in real time is a much more complex problem. Currently, the problem can be simplified somewhat if a small subset of spectral bands that will enable good classification accuracy with minimal data processing is determined. The useful spectral bands are dependent on the investigated food item, and these are usually selected by trial and error or exhaustive search methods. In this study, a faster method is explored, which uses a local discriminant bases (LDB) algorithm to extract the most discriminative features along the spectral- and spatial-frequency axis of the multispectral data for classification. The developed algorithm also identifies the optical filter center frequency and bandwidth (FWHM) that provide optimal discrimination in the multispectral imaging system. This method is validated for detecting contaminated hazelnut kernels and red chili peppers with their multispectral images.

The sample preparation and data acquisition together with data preprocessing are described in Section 2. The developed feature extraction and selection algorithm are described in Section 3. Experimental results and conclusions are given in Sections 4 and 5, respectively.

2. Sample preparation and data acquisition

It is necessary to obtain food samples from both contaminated and uncontaminated classes to identify the difference between the samples. However, it is difficult to find hazelnuts that are naturally contaminated with aflatoxin. There are no formal studies on the probability of incidence of a contaminated hazelnut kernel but for pistachio nuts, it is estimated that incidence of aflatoxin-contaminated nuts is between one in 21,000 and 25,000 nuts (Sommer and Fortlage, 1986). To have an ample number of contaminated nuts for this study, artificially contaminated nuts were used. Unlike hazelnut kernels, aflatoxin-contaminated red chili pepper could be obtained directly from the market.

2.1. Hazelnut kernel preparation

Hazelnuts collected from the “Ordu” region of Turkey during the 2007 harvest were used in this study. The collected nuts were raw (un-roasted) but sun dried down to 6% moisture, which is the moisture level they would be stored at until processing. The hazelnuts were shelled and the hazelnut kernels were divided into three main classes of ‘Untreated Control’, ‘Water Control’ and ‘*A. parasiticus*-Inoculated’. The ‘Untreated Control’ class, is comprised of 104 untreated hazelnuts, which are considered the control group of hazelnuts. A total of 102 hazelnuts, were suspended in pure water for 30 s for ‘Water Control’ to obtain fungal infections from fungal spores naturally present on the hazelnuts and 79 hazelnuts were suspended in an aqueous suspension of *Aspergillus parasiticus* (NRRL 2999) spores for 30 s for ‘*A. parasiticus*-Inoculated’ class. The mold spore concentrations on the ‘*A. parasiticus*-Inoculated’ hazelnuts were in the range of 10^5 – 10^8 spores, depending on the surface area of the kernels. The soaked kernels (*A. parasiticus*-Inoculated and Water Control) were incubated at 28 °C with 90% humidity for nine days, separately. Mold growth was visually observed on all of the incubated hazelnuts, including both ‘*A. parasiticus*-Inoculated’ and ‘Water Control’. Therefore, all were considered fungal contaminated. At the end of day nine, all of the kernels were roasted at 140 °C for 15 min. The roasting process removed the seed coat as well as the mold spores over the kernel surfaces. These hazelnuts were sent for chemical analysis to test for aflatoxin contamination by using liquid chromatography (Senyuva and Gilbert, 2005) after the multispectral images was acquired. Aflatoxin concentrations over 4 ppb were encountered in two of the 104 ‘Untreated Control’, 15 of the 102 ‘Water Control’ and in all of the ‘*A. parasiticus*-Inoculated’ hazelnuts (Table 1). The mean aflatoxin level of the ‘*A. parasiticus*-Inoculated’ hazelnuts is significantly higher than that of the other two classes.

While the method of soaking nuts post harvest to create fungal infection and aflatoxin contamination is obviously not natural, such occurrences do happen in normal hazelnut handling and storage. Hazelnuts have moisture contents of 25–30% or more when harvested; therefore, before storage, they are dried in the sun until their moisture contents are below 6%, at which point they can be stored safely. However, some nuts will not be completely dried and some will be rained on. Nuts are usually quite warm when placed into storage, increasing the possibly some condensation to occur as the grain bin cools and is aerated. This then can create moist pockets in the storage bin where fungi can thrive, while other nuts in the bin are unaffected. Therefore, the method of water soaking nuts to create fungal infection is realistic. Soaking nuts with high amounts of *Aspergillus* spores simulates effect of nuts that may have grown near insect infested nuts and were subjected to considerable mold spore pressure.

2.2. Chili pepper preparation

A total of 40 ground chili pepper samples sold as previously packaged or unpackaged were collected from nine different cities of Turkey. The samples were sent for chemical analysis (Senyuva

Table 1
Number of aflatoxin-contaminated kernels and the mean aflatoxin level (ppb) of the three groups of hazelnuts. ND (aflatoxin <4 ppb), sd = aflatoxin standard deviation.

	≥4 ppb	ND(<4 ppb)	Average
‘Untreated Control’ (104 nuts)	2	102	0.7 ppb (sd:40.4)
‘Water Control’ (102 nuts)	15	87	7.5 ppb (sd:941)
‘ <i>A. parasiticus</i> – Inoculated’ (79 nuts)	79	0	2227 ppb (sd: 1.8. 10 ⁶)

Table 2

Number of aflatoxin-contaminated chili pepper samples and the average aflatoxin level (ppb) of these samples in two groups.

	≥ 10 ppb	ND(<10 ppb)	Average
'UnCont'	0	16	0.7 ppb (sd:40,4)
'Cont'	24	0	7.5 ppb (sd:941)

and Gilbert, 2005) after multispectral imaging (Table 2). The chili pepper samples were assigned to two classes by considering their aflatoxin concentrations with a threshold of 10 ppb, which is the limit defined by EU commission. Samples (16 out of 40) were assigned to the uncontaminated class (*UnCont*), and the remaining 24 samples were assigned to the contaminated class (*Cont*).

Each of the chili pepper samples were also divided into three sub-samples and imaged separately to increase the number of training samples in the experiments. That gave us a total of 120 (= 40 × 3) pepper images to be explored. The sub-samples of five main samples were also chemically analyzed individually to verify that the sub-samples of the main sample have similar aflatoxin contamination levels and would be assigned to same class as contaminated or un-contaminated.

2.3. Multispectral data acquisition

A multispectral imaging system (Fig. 1), including a DMK 41BF02 digital charged coupled device (CCD) camera, two UV-A light sources that have peak intensity at 365 nm, bandpass filters,

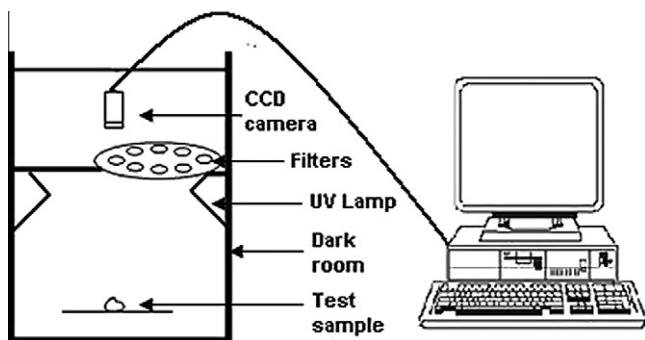


Fig. 1. A schematic diagram of multispectral imaging system.

a filter wheel to hold the filters, a UV cabinet to block ambient light and a computer for recording the images, was used for image acquisition.

Samples are screened with 12 different filters, some at 400–510 nm with 10 nm full width half maximum (FWHM) and others at 550 and 600 nm with 70 and 40 nm FWHM, respectively. The reflected light from the samples was captured and recorded with an IC capture image acquisition tool (The Imaging Source Inc.). The optimal exposure time of the camera was experimentally detected as 0.3 for the hazelnuts samples. However, this time is increased to 2 s for red chili pepper. Pepper samples absorb a larger portion of the incident light and do not reflect sufficient light for camera. A few of the spectral band images for hazelnuts and red chili peppers were shown in Fig. 2 and in Fig. 3, respectively

2.4. Data preprocessing

For the hazelnut images, binary masks were required to extract the hazelnut from the background and the pixels of the regions where the inner skin was not removed during roasting. The images taken at 550 nm were appropriate for mask generation. This band clearly separates the nut from background and unskinned regions. However, other spectral bands could be used as well. The mask was further improved by erosion and dilation operations (Gonzales and Woods, 1992). These morphological operations removed undesired defects due to thresholding. The generated mask was applied to all spectral images of the hazelnut. Instead of a whole hazelnut image, the masked spectral images were divided into square regions (91 × 91 pixels). Each region was regarded as an independent sample and was later used for voting on the class membership of a given hazelnut kernel.

3. Feature extraction and selection

Saito and Coifman (1994) developed the local discriminant bases (LDB) algorithm to obtain localized information for signal and image classification. The LDB algorithm first decomposes the time or frequency axis with a wavelet or trigonometric representation in binary tree format. The nodes in the binary tree are then pruned with their distances between classes. The original LDB algorithm decomposes the time axis by local cosine packets or the frequency axis by wavelet packets. However, Ince et al. (2006) showed that decomposition along two axes (time, frequency) is crucial to get the exact location of discriminating

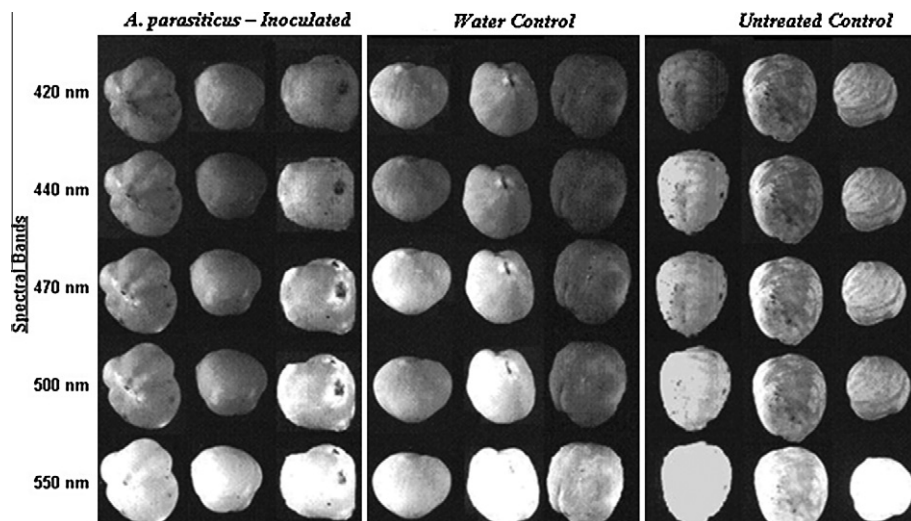


Fig. 2. A few spectral band images for the *A. parasiticus*-Inoculated, Water Control and Untreated Control groups of hazelnuts.

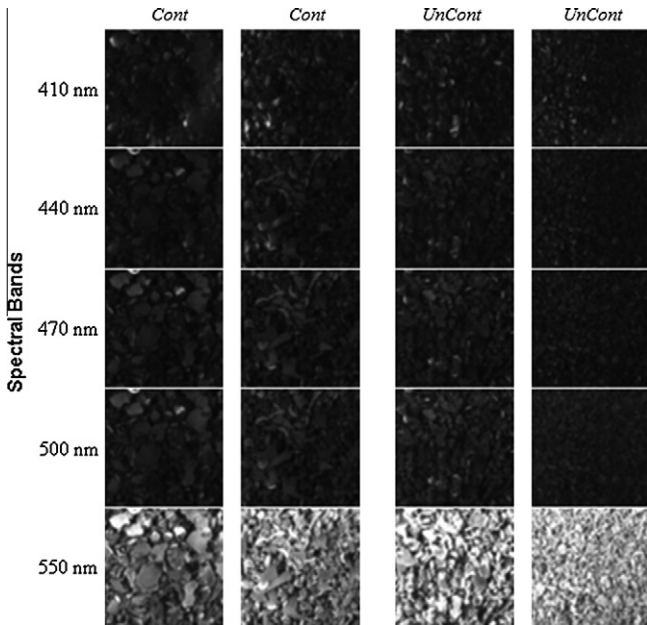


Fig. 3. A few spectral band images of the Cont and UnCont groups of chili pepper samples.

features. The LDB algorithm has previously been adapted to hyperspectral images by representing the hyperspectral curve of pixels as a one-dimensional signal and this signal is decomposed either along the frequency axis (Kumar et al., 2001; Hsu and Tseng, 2002) or along the spectral axis (Cheriyadat and Bruce, 2003).

In this study, the original LDB algorithm is extended to a three-dimensional space in which the two of the dimensions correspond to the spatial-frequency axis and the third dimension is along the spectral axis. The algorithm (Fig. 4) starts with generating two feature trees along the spectral and spatial-frequency axes to localize the features in all three dimensions (spectral and spatial frequency). These trees are then pruned sequentially to extract the most discriminative features for classification. The extracted features are then selected by feature selection algorithms to obtain the highest classification accuracy with the least number of features. The location of the selected features can be used to design a more compact multispectral image acquisition system in which only the specified optical bandpass filters will be employed. In this

way, the highest classification accuracy could be accomplished by a fast and inexpensive image acquisition setup.

3.1. Feature tree generation

The first step in the algorithm is to obtain an energy-based candidate feature set by generating two feature trees along the spectral and spatial-frequency axes sequentially. In the first tree, the reflectance energies $e(i)$ of $S(\leq 2^L)$ spectral images $f_i(x, y)$ of size $M \times N$ are placed on the (lowest) L^{th} level depth of the tree from left to right:

$$e(i) = \frac{1}{MN} \sum_{x=1, y=1}^{MN} |f_i(x, y)| \quad i = 1, 2, \dots, S \quad (1)$$

Fig. 5 illustrates an $L = 4$ binary level spectral band tree having 16 spectral bands (SB). For the case of $S < 2^L$, the remaining nodes at the L^{th} level can be set to null to complete the binary tree. The energy value of the mother nodes $e(\text{mother})$ at the higher levels are assumed to be the sum of the energies of their child nodes.

$$e_L(\text{mother}) = \sum_j e(j) \quad j = 1, 2, \dots, J \quad (2)$$

where J is the number of children of the mother node at level L .

The second feature tree is generated only for each spectral band images (SB1–SB16 in Fig. 5) along the spatial-frequency axis in a quad-tree structure by decomposing the images into h levels of full wavelet subbands as in Fig. 6. Wavelet transforms (Mallat, 1998) retain the original image information and completely represents the image in subbands of (LL, LH, HL and HH), where the first character shows the filtering (low or high) along the row and the second character shows the filtering through the image columns.

3.2. Adaptive pruning in spectral and spatial-frequency axis

The feature extraction step (Fig. 4) includes two consecutive pruning operations first on the feature tree generated along the spectral (Fig. 5) and second on the tree generated on the spatial-frequency axis (Fig. 6). The pruning operation is basically performed by comparing the mother nodes with their children nodes by starting from the bottom level. When compared, the algorithm keeps the mother node if its discrimination value is higher than all of its children. Otherwise, the children nodes survive as nodes with high discrimination potential to be compared at the higher tree level. We used the Euclidean distance between the cumulative

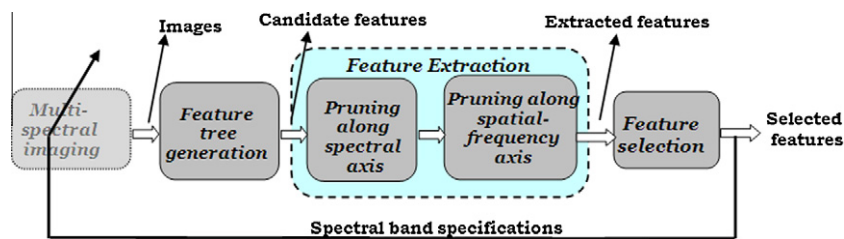


Fig. 4. Block diagram of the proposed LDB based discriminative feature extraction algorithm.

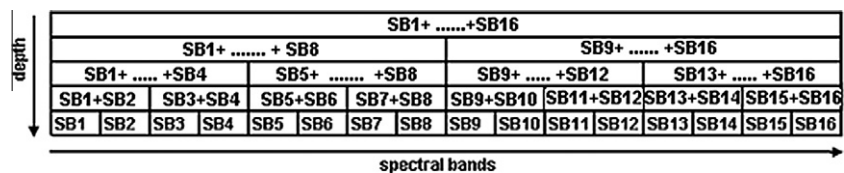


Fig. 5. $L = 4$ binary level spectral band tree.

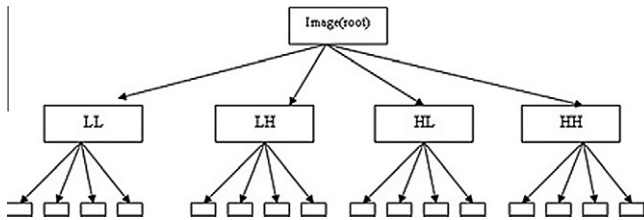


Fig. 6. Full wavelet decomposition quad tree up to $h = 2$ levels.

probability distribution functions (cdf) of the nodes as the discrimination value. However, other distance metrics can be used as well. The first pruning operation may fuse some of the spectral bands to generate the bands with more discriminative potential. To further progress on these generated spectral bands, the wavelet feature trees (Fig. 6) of these merged spectral bands are merged in parallel by averaging to obtain the corresponding spatial-frequency tree for these spectral bands. The second pruning operation is performed along the spatial-frequency axis on these previously generated spectral bands to localize the discriminative information in multi-spectral data. Pruning along the spectral axis has implications on the hardware of the machine vision system since it will reduce the number of optical filters needed and the number of images to be acquired. Pruning along the spatial-frequency axes has implications on the 'signal processing' step which is mainly applied on the images that are already acquired.

3.3. Feature selection and classification

The pruning operations provide the best segmentation in both the spectral- and spatial-frequency axes but do not eliminate the irrelevant features in the tree. Therefore, the extracted features are then sorted by feature selection methods. The algorithm also tracks the location of these features in the data space to make elimination in the data space possible. Different algorithms, including statistical or chemometrics based, could be used for feature subset selection (Clemmensen et al., 2010). However, we used three simple feature selections algorithms; Fisher-based (FFS), wrapper based and forward selection (Hastie et al., 2001) in order to emphasize the feature extraction step. The FFS algorithm, which is an example of a filter model, considers the feature class distances by

$$F = \frac{|\mu_{1k} - \mu_{2k}|}{\sigma_{1k}^2 + \sigma_{2k}^2} \quad (3)$$

where μ_{ik} and σ_{ik} are the mean and variance of the k^{th} feature of the i^{th} class, respectively. The features ranked by the FFS algorithm are incrementally concatenated to the feature vector to obtain the minimum number of features for best classification. Unlike the FFS algorithm, the wrapper-based feature selection algorithm searches for the best feature subset giving the best classification accuracy among all of the subset combinations. In a wrapper-based algorithm, the data of the investigated feature subset is randomly divided into train, validation and test sets. An initial machine learning algorithm is trained with the train set and tested with the validation set. The classification accuracy of the testing gives the merit of the investigated feature subsets and the subset providing the minimum error is selected as the optimal subset. This optimal subset is then tested with an independent test set to evaluate the actual error.

In contrast to the wrapper model, the forward 325 selection starts with a subset including the most discriminative feature. Then this subset is extended incrementally with new features which supply the best combination with the current subset.

In addition to these three feature selection algorithms that were applied on pruned features; we fed the candidate feature directly into the classifier by omitting the pruning step (Fig. 6) for comparison purposes. The candidate features were either all fed directly into the classifier or their dimension is first reduced by Principal Component Analysis (PCA) and then fed into the classifier.

As the classifier, the standard linear discriminant analysis (LDA) was used. This simple classifier was selected to highlight the contribution of the feature extraction step. A more complex classifier like ANN or SVM could give higher classification rates but they could conceal the contribution of the feature extraction.

4. Experimental results

The algorithm is tested for detecting aflatoxin-contaminated red peppers and hazelnut kernels. The hazelnut kernels were also classified as fungal infested (*Infested*) or uninfested (*UnInfested*) without considering the aflatoxin concentration, as described in Section 2.1. The data sets in the experiments were randomly divided into four sets for four fold cross-validation. The algorithm was developed with three sets (training) and tested with the remaining set. The classification results shown are the mean of the fourfold classification when performed for all combinations of training and validation sets.

Initially, feature trees are generated first along the spectral-frequency axis and then along the spatial-frequency axis. The reflectance energies of 12 spectral images (400–510 nm) are placed on the 4th level of the binary tree from left (SB1) to right (SB12) (Fig. 5). The remaining four spectral band nodes (SB13–SB16) at the 4th level are set to null to complete the binary tree. Consequently, the spatial-frequency quad feature tree is generated by decomposing the spectral bands using a full wavelet transform. We used the Daubechies 8-tap filter for decomposition. Other wavelets can be used as well. For each spectral image, a total of 21 subband images were constructed by a two level decomposition (Fig. 6), giving a total of 252 spatial frequency patterns for 12 spectral bands. We used three levels decomposition for chili peppers because it has more textural information than the hazelnuts. That gave us 85 subband images for each spectral band with a total of 1020 features. The pruning along both axes revealed the location of the most discriminative features of the multispectral data. The pruned features are then selected by feature selection algorithms before classification. As an alternative, the 192 (16 × 12) candidate features which were obtained by the 16 lowest level wavelet subband images (Fig. 6) for each 12 spectral band images were fed in classifier directly or after a dimension reduction by PCA. The candidate feature size is 768 (64 × 12) for chili peppers that were obtained by three level wavelet decomposition.

4.1. Classification of fungal infested and uninfested hazelnut kernels

In this problem, the hazelnut kernels are to be categorized into uninfested (*UnInfested*) or fungal-infested (*Infested*) classes using the multispectral images discussed earlier. The ground truth for the categories was based on the treatments: none (*UnInfested*) or water or fungal spore soaking (*Infested*). As stated in Section 2.1, all kernels in the *Infested* category have obvious fungal infection, although the fungi infesting the 'Water Control' class was likely a different species of *Aspergillus*. The kernels that were not treated with water or fungal spore solution followed by incubation were assigned to the *UnInfested* class because there was no sign of fungal infestation. Thus, the 79 '*A. parasiticus*-Inoculated' nuts were added to the 102 'Water Control' nuts to make 181 nuts in the *Infested* class, while 104 'Untreated Control' nuts comprised the *UnInfested* classes.

A total of 12 spectral-frequency features were obtained from 252 features after the pruning operations. We observed that the spectral bands of 440–470 and 480–510 nm are pruned along the spectral axis, and these spectral bands are not decomposed into spatial-frequency subbands. However, the spectral bands of 430 and 440 nm are decomposed into subbands in the spatial-frequency axis. The 12 extracted features are then ranked by feature selection algorithms. The order of features may vary depending on the feature selection algorithm, and this selection may affect the classification accuracy. The selected features were fed into a linear classifier one by one and the lowest classification errors of 4.34% and 5.45% were obtained by five Fisher based and wrapper-selected features, respectively (Table 3). For the candidate feature set, the accuracies of 6.37% and 8.69% were achieved by using all 192 features or five PCA component obtained by projecting of all 192 features, respectively.

When individual kernel classification results using the five FFS features were analyzed, it was observed that 10 of the 181 *Infested* hazelnuts and three of the 104 *UnInfested* hazelnuts were misclassified. However, none of the misclassified *Infested* hazelnuts contained aflatoxin above 4 ppb. The mean aflatoxin level of the test set, including hazelnuts from both the *Infested* and *UnInfested* groups, was 608 ppb, and the algorithm classified the kernels into two classes whose average aflatoxin contamination levels were 1095 and 0.7 ppb.

4.2. Classification of aflatoxin-contaminated and uncontaminated hazelnut kernels

In this problem, the hazelnuts are categorized by assigning the kernels with over 4 ppb aflatoxin concentration to *Afla+* and the remaining kernels to the *Afla-* group without considering their fungal infestation (Table 1). There are a total of 96 *Afla+* class kernels, of which two are from the 'Untreated Control' class, 79 are from the '*A. parasiticus*-Inoculated' class and 15 are from the 'Water Control' class, and 189 *Afla-* group hazelnuts, of which 102 are from the 'Untreated Control' class and 87 are from the '*A. parasiticus*-Inoculated' class. The average aflatoxin levels of the *Afla+* and *Afla-* are 1883 and 0.06 ppb, respectively. For this data set, the spectral pruning in the feature extraction step pruned the spectra bands of 420–430, 440–450 and 480–510 nm but kept the spectral bands of 400, 410, 460 and 470 nm intact. The subbands in the spatial-frequency axis of all spectral bands are completely pruned except for the 420–430 nm spectral bands. The selected features are fed into the linear classifier with four fold validation. However, lower classification accuracies (Table 4) are obtained compared with the classification of the *Infested* and *UnInfested* classes (Section 4.1).

A minimum accuracy of 10.34% was achieved with four Fisher selected features. The PCA gave the same error with four components. However, it used all 192 features for getting these four components. When the classification results with the four FFS-selected

Table 3
Classification error with pruned and unpruned (candidate) features for the fungal infested hazelnut kernel separation.

	Feature selection/ reduction Method	Number of features	Classification error (%)
Candidate feature set (192)	PCA	5	8.69
	No reduction	192	6.37
Pruned feature set (12)	Fisher (FFS)	5	4.34
	Forward selection	5	7.23
	Wrapper	5	5.44

Bold number indicates the minimum error among the others.

Table 4
Classification error with pruned and unpruned (candidate) features for the aflatoxin contaminated hazelnut kernel separation.

	Feature selection/ reduction Method	Number of features	Classification error (%)
Candidate feature set (192)	PCA	4	10.34
	No reduction	192	15.31
Pruned feature set (12)	Fisher	4	10.34
	Forward selection	4	10.87
	Wrapper	4	10.96

Bold number indicates the minimum error among the others.

Table 5
The classification error curves on FFS- and Wrapper-based feature selected features for chili pepper separation problem.

	Feature selection/ reduction method	Number of features	Classification error (%)
Candidate feature set (768)	PCA	6	47.56
	No reduction	768	32.63
Pruned feature set (12)	Fisher	6	20.83
	Forward selection	6	26.38
	Wrapper	6	20.83

Bold number indicates the minimum error among the others.

features are analyzed, it was observed that the algorithm misclassified 3 of the 96 *Afla+* hazelnuts and 39 of the 189 *Afla-* hazelnuts. The average aflatoxin level of the tested hazelnuts decreased to 0.84 ppb from the group average of 608 ppb by removal of the *Afla+* hazelnuts. Therefore, it is recommended to separate *Infested* kernels from hazelnut lots to decrease aflatoxin levels because the contaminated kernels that are obtained by soaking in pure water ('Water Control') are likely to contain aflatoxin. Additionally, fungal infested nuts are not preferred by consumers.

4.3. Classification of aflatoxin-contaminated and uncontaminated red chili peppers

In this problem, the pepper samples are categorized into *Afla+* and *Afla-* classes. Of the pepper samples, 72 having aflatoxin concentrations over 10 ppb were assigned to the *Afla+* class, and the remaining 48 samples were assigned to the *Afla-* class. The pruning operation in feature extraction step pruned the spectral bands of 400–430, 440–470 and 500–510 nm; however kept the spectral bands of 480 and 490 nm intact. The subbands in the spatial-frequency axis of the 400–470 nm spectral bands are completely pruned. The extracted features were then selected and fed into classifier. The feature map above is obtained by leave-one out principle for chili pepper.

The lowest classification errors of 20.83% were obtained with six wrapper- and FFS-selected features (Table 5). However, the highest classification error was obtained with six PCA features.

When the classified results with the six wrapper-based feature selection ordered features are analyzed, it is observed that 9 of the 72 *Afla+* peppers and 15 of the 48 *Afla-* peppers are misclassified. The mean aflatoxin level of samples decreased to 22.85 ppb from the group average of 38.26 ppb by separation of the aflatoxin-contaminated pepper samples.

5. Conclusions

An LDB-based feature extraction and selection algorithm for the analysis of hyperspectral data along the spectral and spatial-frequency axes is developed. The algorithm was implemented on consecutive multispectral images. The developed algorithm

extracts the relevant features of the data and adaptively decreases the feature dimension and the corresponding data by pruning in feature space. The pruning operation along the spectral axis identified a small subset of optical filters required for a high speed image acquisition system. The features giving the highest classification accuracy can be extracted from only two or three spectral bands, which make the design of practical food inspection and sorting systems simple and effective. The developed algorithm was tested on detection of contaminated hazelnuts and red chili peppers. The algorithm classified the red chili peppers into aflatoxin-contaminated and uncontaminated classes with 79.17% accuracy so that the aflatoxin level of the test set is decreased to 22.85 from 38.26 ppb by the removal of the ones that are classified as aflatoxin-contaminated. The hazelnut kernels are independently subjected to two different classifications: first, on the detection of aflatoxin-contamination and, second, on the detection of fungal infestation without considering their aflatoxin concentrations. A correct classification accuracy of 92.3% is achieved for classifying the hazelnuts as aflatoxin-contaminated (>4 ppb) or not (<4 ppb). Better classification accuracy of 95.67% is achieved for classifying the hazelnuts as fungal infested or not. The average aflatoxin level of the tested hazelnuts is decreased to 0.84 and 0.7 ppb from 608 ppb by removal of the ones detected as aflatoxin-contaminated and fungal infested, respectively. It is recommended to separate fungal infested (*Infested*) kernels from hazelnut lots to decrease the aflatoxin level because the fungal infested kernels are the high risk ones, and these nuts are also not preferred by consumers.

Acknowledgements

This work is supported by the National Scientific Research Council of Turkey (TUBITAK) project EEEAG-106E057.

References

- Bollenbacher, K., Marsh, P.B., 1954. A preliminary note on a fluorescent-fiber condition in raw cotton. *Plant Disease Reporter* 38, 375–379.
- Bothast, R.J., Hesseltine, C.W., 1975. Bright greenish-yellow fluorescence and aflatoxin in agricultural commodities. *Applied Microbiology* 337, 338.
- Cheriyadat A., Bruce L. M., 2003. Decision level fusion with best-bases for hyperspectral classification. *IEEE Workshop on Advances in Techniques for Analysis of Remotely Sensed Data*, USA.
- Clemmensen, L.H., Hansen, M.E., Ersboll, B.K., 2010. A comparison of dimension reduction methods with application to multi-spectral images of sand used in concrete. *Machine Vision and Applications* 21, 959–968.
- Dichter, C.R., 1984. Risk estimates of liver cancer due to aflatoxin exposure from peanuts and peanut products. *Food and Chemical Toxicology* 22 (6), 431–437.
- Doster, M.A., Michailides, T.J., 1998. Production of bright greenish yellow fluorescence in figs infected by *Aspergillus* species in California orchards, The American Phytopathological Society. *Plant Disease* 82 (6).
- European Commission Regulation (EC) No 1881/2006 of 19 December 2006: setting maximum levels for certain contaminants in foodstuffs, *Official Journal of European Union*.
- Fersaie, A., McClure, W.F., Monroe, R.J., 1978. Development of indices for sorting Iranian pistachio nuts according to fluorescence. *Journal of Food Science* 43 (5), 1550–1552.
- Gonzales, R.C., Woods, R.E., 1992. *Digital Image Processing*, 3rd ed. Addison-Wesley Pub (SD).
- Hadavi, E., 2005. Several physical properties of aflatoxin-contaminated pistachio nuts: application of BGY fluorescence for separation of aflatoxin-contaminated nuts. *Food Additives and Contaminants* 22 (11), 1144–1153.
- Hastie, T., Tibshirani, R., Friedman, J., 2001. *The Elements of Statistical Learning*. Springer.
- Hirano, S., Okawara, N., Narazaki, S., 1998. Near infrared detection of internally moldy nuts. *Bioscience, Biotechnology, and Biochemistry* 62 (1), 102–107.
- Hsu, P.H., Tseng, Y.H., 2002. Feature extraction of hyperspectral data using the best wavelet packet basis, *Proc. IEEE Geoscience and Remote Sensing Symposium (IGARSS)*.
- Ince, N.F., Arica, S., Tewfik, A.H., 2006. Classification of single trial motor imagery EEG recordings with subject adapted non-dyadic arbitrary time-frequency tilings. *Journal of Neural Engineering* 3, 235–244.
- Jacks, T., 2005. Evaluation of kojic acid for determining heme and nonheme haloperoxidase activities spectrophotometrically. *Analytical Letters* 38, 921–927.
- Kumar, S., Ghosh, J., Crawford, M.M., 2001. Best-bases feature extraction algorithms for classification of hyperspectral data. *IEEE Transactions on Geoscience and Remote Sensing* 39, 1368–1379.
- Mallat, S.G., 1998. *A Wavelet Tour of Signal Processing*. Academic Press.
- Marsh, P.B., Simpson, M.E., Ferretti, R.J., Campbell, T.C., Donoso, J., 1969. The relation of aflatoxin in cotton seeds at harvest to fluorescence in fiber. *Journal of Agricultural and Food Chemistry* 17, 462–467.
- Pearson, T., Wicklow, D., Maghirang, E., Xie, F., Dowell, F., 2001. Detecting aflatoxin in single corn kernels by using transmittance and reflectance spectroscopy. *Transactions of the ASAE* 44 (5), 1247–1254.
- Saito, N., Coifman, R.R., 1994. Local discriminant bases, in *mathematical imaging: wavelet applications in signal and image processing*. *Proceedings of SPIE* 2003, 2–14.
- Schatzki, T.F., Pan, J.L., 1996. Distribution of Aflatoxin in Pistachios. 3. Distribution in Pistachio Process Streams. *Journal of Agricultural and Food Chemistry* 44, 1076–1084.
- Senyuva, H.S., Gilbert, J., 2005. Immunoaffinity column cleanup with liquid chromatography using post-column bromination for determination of aflatoxins in hazelnut paste: interlaboratory study. *Journal of AOAC International* 88, 2.
- Sommer, N.F., Fortlage, R.J., 1986. Relation of early splitting and tattering of pistachio nuts to aflatoxin in the orchard. *Phytopathology* 76, 692–694.
- Steiner, W.E., Rieker, R.H., Battaglia, R., 1988. Aflatoxin contamination in dried figs: distribution and association with fluorescence. *Journal of Agricultural and Food Chemistry* 36 (1).
- Steiner, W.E., Brunschweiler, K., Leimbacher, E., Schneider, R., 1992. Aflatoxins and fluorescence in Brazil nuts and pistachio nuts. *Journal of Agricultural and Food Chemistry* 40, 2453–2457.
- Tayson, T.W., Clark, R.L., 1974. An investigation of florescence properties of the aflatoxin -infected pecans. *Transactions of the ASAE* 17, 942–944.
- Wicklow, D., 1999. Influence of *Aspergillus flavus* strains on aflatoxin and bright greenish yellow fluorescence of corn kernels, *The American Phytopathological Society. Plant Disease* 83 (2), 1–4.
- Wilson, D., 1989. Analytical method for aflatoxin in corn and peanuts, *Arch. Environment Contamination and Toxicology* 18, 304–314.